FLEXURAL STRENGTHENING OF URM WALLS WITH FRP LAMINATES

J. Gustavo Tumialan, University of Missouri-Rolla, Rolla, MO

Antonio Morbin, University of Padova, Italy

Francesco Micelli, University of Lecce, Italy

Antonio Nanni, University of Missouri-Rolla, Rolla, MO

Abstract

Unreinforced masonry (URM) walls are prone to failure when subjected to out-of-plane loads caused by earthquakes or high wind pressures. This paper presents the results of an experimental program on the flexural behavior of URM walls strengthened with externally bonded FRP laminates. Twenty-six URM specimens (concrete and clay masonry) were tested. The specimens were strengthened with different amounts of reinforcement to observe their improved performance and the mode of failure. Two types of FRP fabrics, glass (GFRP) and aramid (AFRP), were used. Also, the influence of the putty filler on the bond strength was investigated. Strength and pseudo-ductility of URM walls were significantly increased by strengthening with FRP laminates. The test results made possible to identify three basic modes of failure: one, shear failure, related to the parent material (i.e. masonry); and the remaining two associated with the reinforcing material, debonding and rupture of FRP, respectively. Based on experimental evidence, the paper provides criteria that can be used in the development of design guidelines.

Introduction

Structural weakness, overloading, dynamic vibrations, settlements, and in-plane and out-of-plane deformations can cause failure of unreinforced masonry (URM) structures. URM buildings have features that, in case of overstressing, can threaten human lives. These include unbraced parapets, inadequate connections to the roof, floor and slabs, and the brittle nature of the URM elements. Organizations such as The Masonry Society (TMS) and the Federal Emergency Management Agency (FEMA) have determined that failures of URM walls result in more material damage and loss of human life during earthquakes than any other type of structural element. This was evident from the post-earthquake observations in Northridge, California (1994) and Izmit, Turkey (1999) (see Figure 1).

Fiber reinforced polymer (FRP) composites may provide viable solutions for the strengthening of URM walls subjected to in-plane and out-of-plane loads caused by high wind pressures or earthquakes. The use of FRP materials offers important advantages in addition to their mechanical characteristics and ease of installation. For example, disturbance to occupants is minimized and, during installation, there is a minimal loss of usable space. Furthermore, from the structural point of view, the dynamic properties of the structure remain unchanged because there is no addition of mass. For the case of stiffness, the designer may select not to affect it, so that there is no redistribution of forces.

This paper presents the results of an experimental program on the flexural behavior of URM walls strengthened with externally bonded FRP laminates. The specimens consisted of concrete and

clay masonry panels strengthened with different amounts of FRP reinforcement to observe their improved performance and the mode of failure. Two types of FRP fabrics, glass FRP (GFRP) and aramid (AFRP), were used for the strengthening. In addition, the influence of the putty filler on the bond strength was investigated. The putty is used to fill small surface voids and to provide a leveled surface to which the FRP can be attached. Based on experimental evidence generated by this investigation and others, the paper provides criteria that can used in the development of design guidelines when a masonry wall is assumed to be simply supported (i.e. arching mechanism is not present).

Figure 1. Out-of-Plane Failure (Izmit, Turkey, 1999)

Experimental Program

Test Matrix

Table 1 summarizes the characteristics of 25 masonry specimens that were constructed for this experimental program. Twelve walls were built with concrete blocks and the remaining 13 with clay bricks. Their nominal dimensions were 600 mm (24 in.) wide by 1200 mm (48 in.) high. The nominal wall thickness was about 95 mm (3.75 in.) The test specimens were strengthened with GFRP and AFRP laminates. Two different masonry units (concrete and clay), and two surface preparation methods (with or without putty filler) were investigated to account for different compressive strengths and surfaces. The surface preparation of all the masonry specimens built with clay units included the use of putty. This was because the clay brick wall surfaces exhibited more unevenness that those of the concrete blocks.

The two different FRP systems (GFRP and AFRP) were installed by manual lay-up in different amounts to observe the wall performance and mode of failure. All the masonry panels were strengthened with a single FRP strip placed along the longitudinal axis. The strip widths ranged from 75 mm (3 in.) to 300 mm (12 in.) on the tension side. Table 2 provides an indication of the amount of FRP reinforcement, $\rho_f = \text{fiberarea}/(\text{wallwidth} \times \text{wallthickness})$ for specimens in this program and others. Due to the brittle nature of URM it is meaningless to test an unstrengthened wall. Four series of walls were tested: COC, COA, CLG, and CLA. The first two characters in the code represent the type of masonry used, “CO” for concrete masonry and “CL” for clay masonry. The third character represents the type of fiber, “G” for GFRP and “A” for AFRP. The last character indicates the width of the strip in

inches. Thus, CLG5 is a clay masonry wall, strengthened with a GFRP laminate, having a width of 125 mm (5 in.) The character "R" indicates a test repetition. In every case, the length of the FRP strips was 1170 mm (46 in.), in this manner the laminate would not touch the roller supports used for testing.

Table 1. Test Matrix

Masonry Type	**Series**	**FRP Fiber**	**25 Specimen Codes**				
			FRP Strip Width, mm (in.)				
			75 (3)	125 (5)	175 (7)	225 (9)	300 (12)
Concrete	COG	GFRP	COG3 COG3R	COG5 COG5R	COG7	COG9	COG12
	COA	AFRP	COA3	COA5	COA7	COA9	COA12
Clay	CLG	GFRP	CLG3 CLG3R	CLG5 CLG5R	CLG7 CLG7R	CLG9	CLG12
	CLA	AFRP	CLA3	CLA5	CLA7	CLA9	CLA12

Materials

Tests were performed to characterize the engineering properties of the materials used in this investigation. The average compressive strengths of concrete and clay masonry obtained from the testing of prisms (ASTM C1314) were 10.5 MPa (1520 psi) and 17.1 MPa (2480 psi), respectively. Standard mortar specimens were tested according to ASTM C109. An average value of 7.6 MPa (1100 psi) at an age of 28 days was found; therefore, the mortar can be classified as Type N (Wideman, 1994).

Tensile tests were performed on FRP laminates to determine their engineering properties, which are related to fiber content and not to composite area. The FRP coupons had a width of 37.5 mm (1.5 in.) and gage length of 250 mm (10 in). The fiber thickness was 0.35 mm (0.014 in.) for glass and 0.28 mm (0.011 in.) for aramid. In order to provide appropriate anchorage during testing, rectangular GFRP tabs were used at both ends of each coupon to diffuse the clamping stresses. The tabs were made of two GFRP layers and were glued using the same resin used for the manual lay-up. Their dimensions were 51.0 mm (2 in.) by 38.1 mm (1.5 in.). Details of coupon fabrication and testing procedure are shown elsewhere (Yan, 2001). The test results showed that the tensile strength of GFRP was equal to 1690 MPa (245 ksi) and the modulus of elasticity was 92.9 GPa (13460 ksi). In the case of AFRP, the tensile strength was 1876 MPa (272 ksi) and the modulus of elasticity was equal to 115.2 GPa (16700 ksi).

Test Setup

The walls were tested under simply supported conditions (see Figure 2). A 12 ton (26.4 kips) capacity hydraulic jack activated by a manual pump was used to load the specimen. The force generated by the hydraulic jack was transferred to the specimen by means of a steel beam supported by two rollers, which applied a load along two lines spaced at 200 mm (8 in.) The load was applied in cycles of loading and unloading. An initial cycle for a low load was performed in every wall to verify that both the mechanical and electronic equipment were working properly. The data acquired by the load cell, Linear Variable Differential Transducers (LVDTs) and strain gauges were collected by a data acquisition system at a frequency of 1.0 Hz. A total of six LVDTs were used to register deflections. Two LVDTs were placed at midspan, in both sides of the specimen, two were located at the fourths of the masonry

panels. The remaining two were located at the supports to register settlements. Five strain gauges were placed in the FRP laminates of specimens COG3R, COG5R, CLG3R, CLG7R, and CLG5R. One strain gauge was placed at midspan, two strain gauges were placed at 200 mm (8 in.) and two at 400 mm (16 in.) from each wall end.

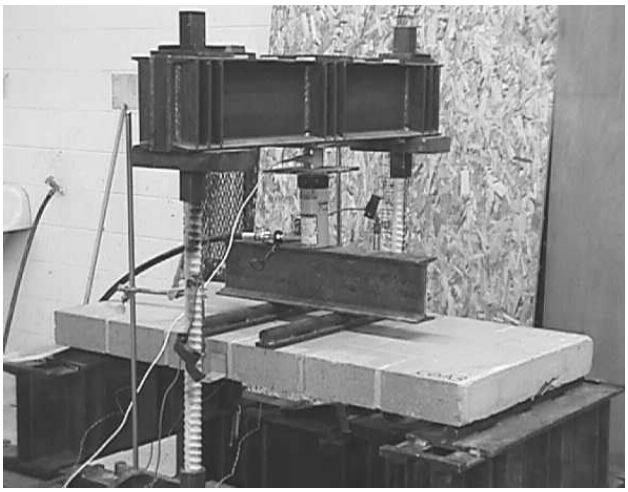

Figure 2. Test Setup

Test Results

Modes of Failure

The walls exhibited the following modes of failure: (1) debonding of the FRP laminate from the masonry substrate, (2) flexural failure (i.e. rupture of the FRP laminate in tension or crushing of the masonry in compression), and (3) shear failure in the masonry near the support.

FRP Debonding: due to shear transfer mechanisms at the interface masonry/FRP laminate, debonding of the laminate from the masonry substrate may occur before flexural failure (see Figure 3a). Debonding starts from flexural cracks at the maximum bending moment region and develops towards the supports. Since the tensile strength of masonry is lower than that of the epoxy resins, the failure line is in the masonry. In the case of concrete masonry walls, part of the concrete block faceshell remained attached to the FRP laminate.

Flexural Failure: after developing flexural cracks primarily located at the mortar joints, a wall failed by either rupture of the FRP laminate or masonry crushing. FRP rupture occurred midspan (see Figure 3b). The compression failure was manifested by crushing of mortar joints.

Shear Failure: cracking started with the development of fine vertical cracks at the maximum bending region. Thereafter two kinds of shear failure were observed: flexural-shear and sliding shear (see Figures 3c and 3d, respectively). The former was oriented at approximately 45^{o}, and the latter occurred along a bed joint causing sliding of the wall at that location, typically, at the first mortar joint in walls heavily strengthened. In the flexural-shear mode, shear forces transmitted over the crack caused a differential displacement in the shear plane which resulted in FRP debonding.

(a) FRP Debonding (COG5)

(b) FRP Rupture (CLA5)

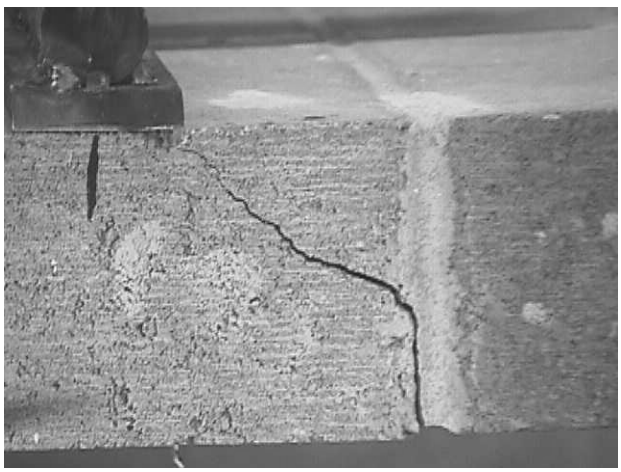

(c) Flexural-Shear (COA9)

(d) Sliding Shear (CLG12)

Figure 3. Modes of Failure

Discussion of Results

Figure 4 illustrates the moment vs. deflection curves for the concrete and clay masonry series COG, COA, CLG and CLA. It is observed that the strength and stiffness of the FRP strengthened walls increased dramatically when comparing them to a URM specimen. According to the Masonry Standards Joint Committee (MSJC, 1999), the allowable flexural tension for concrete and clay masonry for a Type N mortar can be taken as 262 kPa (38 psi) and 414 kPa (60 psi), respectively. Considering that the nominal strength is approximately 2.5 times the allowable one, the nominal moments at cracking for the concrete specimens can be estimated as 0.45 kN-m (0.33 ft-kips), whereas for the clay specimens this value is 0.95 kN-m (0.70 ft-kips). This indicates that depending on the amount of FRP, increments ranging from 4 to 14 times of the original masonry capacity were achieved. Since masonry possesses a significant amount of variability attributed to labor and materials, this range of values should be taken simply as a reference.

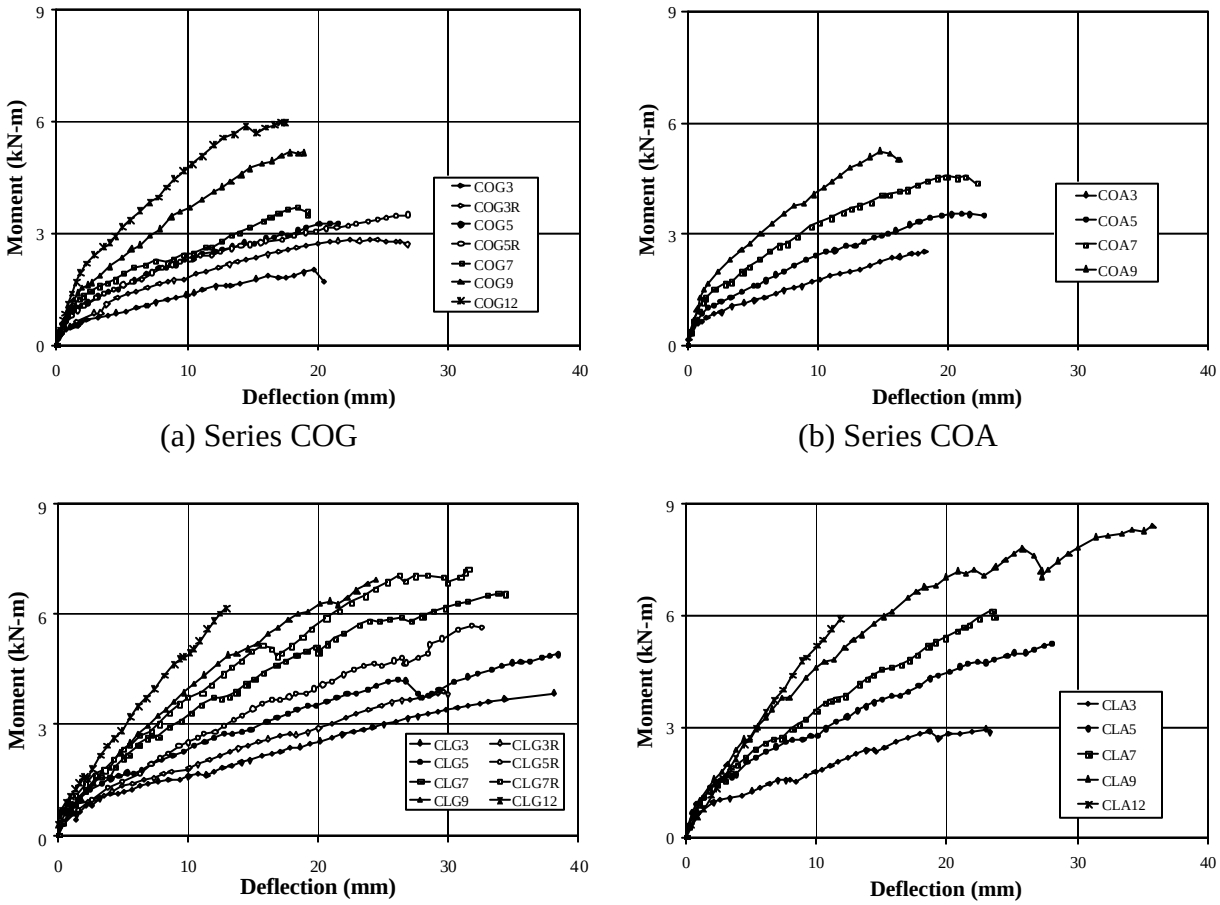

(a) Series COG (b) Series COA

(c) Series CLG (d) Series CLA

Figure 4. Moment vs. Deflection Curves

The test results show a clear and consistent pattern. Up to cracking the walls behaved almost in linear fashion. Initial cracking occurred at the interface of mortar and masonry for concrete masonry and in the mortar joint itself for clay masonry. Initial cracking was delayed due to the presence of FRP reinforcement. Following this, cracking at the adjacent joint occurred until almost every joint in the high moment bending area was cracked. After cracking, the flexural stiffness is a function of the amount of FRP. A degradation of stiffness that is larger in walls with high amount of FRP reinforcement is observed. In this phase of the test, the cracks widen until the failure occurs.

Rupture of the FRP laminate was observed only in four clay masonry specimens CLA4, CLG3R, CLG5R, and CLA9. This can be attributed to improved bond characteristics provided by the putty. Even though FRP rupture is a desirable mode of failure, there is no certainty that it can be achieved all the time. This was evident from the test results of specimens built with the same masonry units and having the same amount of reinforcement (CLG3 and CLG3R, and CLG5 and CLG5R). Debonding was observed in specimens CLG3 and CLG5; whereas, FRP rupture was registered in specimens CLG3R and CLG5R.

Shear failure was observed in specimens with large amounts of FRP reinforcement. Increments in out-of-plane capacity were also observed in walls failing in a flexure-shear mode. However, some specimens such as CLG9, CLG12 and CLA12 failed due to sliding shear. The test results showed that due to the nature of the sliding shear failure, the overall capacity was less than that registered in similar walls strengthened with a lower amount of reinforcement.

The strains in concrete masonry walls failing by FRP debonding (COG3R and COG5R) averaged 1.4% which represented about 67% of the ultimate strain of GFRP. In the case of the clay masonry, three specimens were instrumented with strain gauges. The reading in the one failing due to debonding (CLG7R) was 1.54%, which is about 73% of the ultimate strain. The remaining two failed due to rupture of the laminate. When FRP failed, the recorded ultimate strain values were similar to those obtained from tensile tests of GFRP laminates (1.82%). Table 2 includes the maximum flexural moments generated by the out-of-plane load as well as the developed strains in the instrumented walls.

Basis for a Design Approach

Of the three modes of failure described, the results obtained in this study and in those shown in the literature (Velazquez, 1998, Roko et al. 1999, Albert et al., 2001, and Hamilton et al., 2001) suggest that the controlling mode is mostly debonding of the FRP laminate. If a large amount of FRP is provided, shear failure may be observed. Debonding may have a direct relationship with the porosity of the masonry surface, which is characterized by the initial rate of absorption tests. It is understood that masonry surface also refers to surfaces prepared with putty. Roko et al. (1999) observed that the absorption of the epoxy is limited in the extruded brick units as compared to the absorption in molded bricks. This is attributed to the glazed nature of their surface, which leads to a reduction of the bond strength between the FRP laminate and the masonry surface.

Figure 5 illustrates the relationship between the experimental-theoretical flexural capacity ratio, and the reinforcement ratio ω_f, expressed as $\rho_f E_f / f'_m (h/t)$, for masonry walls strengthened with a variety of FRP laminates (ρ_f is the amount of FRP, E_f is the modulus of elasticity of FRP, f'_m is the masonry compressive strength, and h/t is the wall slenderness ratio). The experimental data used for plotting Figure 5 were obtained from previous investigations (Albert et al., 2001, Hamilton et al., 2001 and Tumialan, 2001) and from the specimens tested during this investigation. In Figure 5a, data on concrete masonry specimens (without putty) is presented. Figure 5b shows data on clay masonry specimens where the surface has been leveled with putty. The introduction of the slenderness ratio h/t is justified since this parameter is identified as one of the most influential in the out-of-plane behavior of masonry walls. The slenderness ratio and the out-of-plane capacity are inversely proportional. As the slenderness ratio decreases, the out-of-plane strength becomes larger (Angel et al., 1994). Since the out-of-plane strength is directly proportional to the compressive strength, then the slenderness ratio and the compressive strength are inversely proportional. Therefore, it is reasonable to express the relation between the compressive strength and the slenderness ratio as a product.

The database includes specimens built with clay and concrete masonry units strengthened with AFRP, GFRP and carbon FRP (CFRP) laminates. Mostly, the tests showed that the strengthened specimens failed due to debonding of the laminate. The characteristics of the specimens being considered as well as experimental and theoretical flexural and shear capacities used to develop Figure 5 are presented in Table 2. The theoretical flexural capacity of an FRP strengthened masonry wall can be determined based on strain compatibility, internal force equilibrium, and the controlling mode of failure. Theoretical flexural capacities of the strengthened walls were estimated based on the assumption that no premature failure was to be observed. This means that either rupture of the laminate or crushing of masonry would control the wall behavior. For simplicity and similarly to the flexural analysis of RC members, a parabolic distribution was used for compressive stresses in the computation of the flexural capacity of the strengthened walls. According to MSJC (1999) the maximum usable strain ε_{mu} was considered to be 0.0035 mm/mm (in./in.) for clay masonry, and 0.0025 mm/mm (in./in.) for concrete masonry. The tensile strength of masonry was neglected.

Table 2. Experimental and Theoretical Results

Source	Masonry		FRP		Flexure			Shear		Failure
	Type	h/t	System	ρ_f	M_{exp} (kN-m)	M_{the} (kN-m)	ε_f (%)	V_{exp} (kN)	V_{the} (kN)	
COG3	CO	12.3	GFRP	0.0005	2.05	4.18	NA	4.27	11.37	D
COG3R	CO	12.3	GFRP	0.0005	3.22	4.18	1.49	5.52	11.37	D
COG5	CO	12.3	GFRP	0.0008	3.33	5.64	NA	6.89	11.37	D
COG5R	CO	12.3	GFRP	0.0008	5.37	5.64	1.23	7.16	11.37	D
COG7	CO	12.3	GFRP	0.0011	3.74	6.51	NA	7.74	11.37	D
COG9	CO	12.3	GFRP	0.0014	5.23	7.23	NA	10.85	11.37	F-S
COG12	CO	12.3	GFRP	0.0019	6.06	8.12	NA	12.59	11.37	F-S
COA3	CO	12.3	AFRP	0.0004	2.54	3.66	NA	5.25	11.37	D
COA5	CO	12.3	AFRP	0.0006	3.57	5.57	NA	7.38	11.37	D
COA7	CO	12.3	AFRP	0.0009	4.66	6.44	NA	9.70	11.37	F-S
COA9	CO	12.3	AFRP	0.0011	5.25	7.16	NA	10.90	11.37	F-S
COA12	CO	12.3	AFRP	0.0015	6.33	8.05	NA	13.12	11.37	F-S
CLG3	CL	12.3	GFRP	0.0005	3.23	4.23	NA	7.78	22.98	D
CLG3R	CL	12.3	GFRP	0.0005	3.88	4.23	2.25	8.05	22.98	R
CLG5	CL	12.3	GFRP	0.0008	4.89	6.97	NA	10.14	22.98	D
CLG5R	CL	12.3	GFRP	0.0008	5.37	6.97	1.97	11.56	22.98	R
CLG7	CL	12.3	GFRP	0.0011	6.58	9.57	NA	13.61	22.98	D
CLG7R	CL	12.3	GFRP	0.0011	7.20	9.57	1.54	14.63	22.98	D
CLG9	CL	12.3	GFRP	0.0014	6.94	11.09	NA	14.37	14.81	S-S
CLG12	CL	12.3	GFRP	0.0019	6.16	12.47	NA	12.77	14.81	S-S
CLA3	CL	12.3	AFRP	0.0004	2.94	3.70	NA	6.09	22.98	D
CLA5	CL	12.3	AFRP	0.0006	5.23	6.10	NA	10.85	22.98	R
CLA7	CL	12.3	AFRP	0.0009	6.13	8.45	NA	12.72	22.98	D
CLA9	CL	12.3	AFRP	0.0011	8.45	10.66	NA	17.48	22.98	D
CLA12	CL	12.3	AFRP	0.0015	5.90	12.35	NA	12.23	14.81	S-S
Albert et al.	CO	19.2	GFRP	0.0008	21.14	35.52	0.69	18.01	36.93	D
Albert et al.	CO	18.6	CFRP	0.0003	29.50	40.86	0.78	25.13	37.08	D
Albert et al.	CO	18.6	CFRP	0.0003	24.48	40.86	0.73	20.86	50.17	D
Albert et al.	CO	18.6	CFRP	0.0002	12.28	21.24	0.78	10.45	50.17	R
Hamilton et al.	CO	8.6	GFRP	0.0002	3.44	5.46	NA	7.92	25.86	D
Hamilton et al.	CO	8.6	GFRP	0.0002	4.23	5.46	NA	9.74	22.54	R
Hamilton et al.	CO	8.6	GFRP	0.0002	4.89	5.46	NA	11.30	25.86	R
Hamilton et al.	CO	8.6	GFRP	0.0002	5.45	5.46	NA	12.54	22.54	R
Hamilton et al.	CO	22.7	GFRP	0.0008	15.60	21.14	NA	13.48	26.48	R
Hamilton et al.	CO	22.7	GFRP	0.0008	19.35	21.38	NA	16.72	25.24	R
Tumialan	CO	6.0	GFRP	0.0005	11.33	20.86	0.72	25.66	24.06	F-S
Tumialan	CO	6.0	AFRP	0.0005	10.10	22.51	0.82	22.91	24.06	F-S

Legend: D: FRP Debonding R: FRP Rupture
F-S: Flexural Failure S-S: Sliding Shear

The theoretical shear capacity was computed based on the MSJC (1999) recommendations. Thus for all the walls failing in shear, with the exception of those failing due to sliding shear, the shear capacity was estimated based on a shear stress of $3.9\sqrt{f'_m}$, f'_m in MPa ($1.5\sqrt{f'_m}$, f'_m in psi). For walls failing due to shear sliding (CLG9, CLG12 and CLA12), the shear capacities were calculated based on a shear stress of 0.25 MPa (37 psi). This shear stress value is recommended by the MSJC (1999) for masonry in running bond that is not grouted solid. For every wall, the net cross section was used for the computation of the shear capacity. In general, the experimental and theoretical results showed a good agreement (see Table 2).

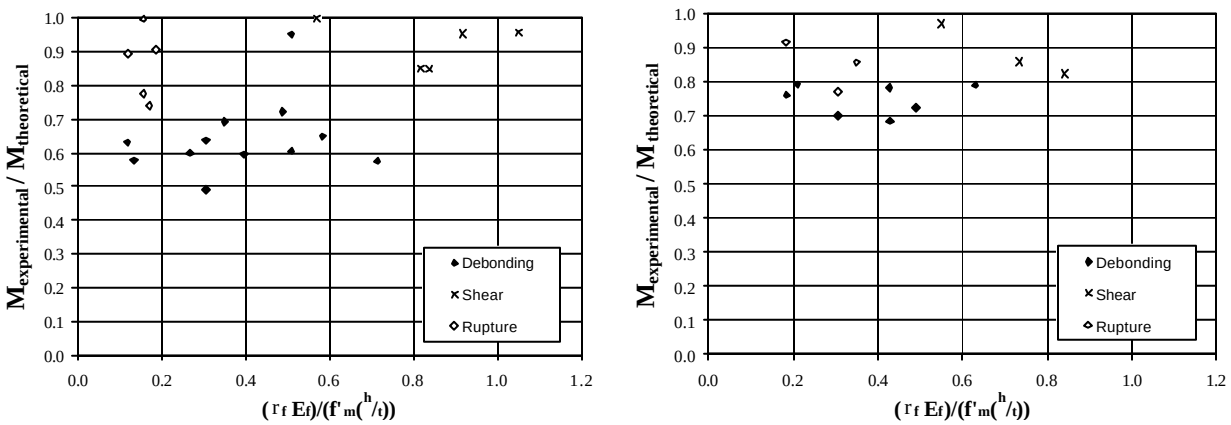

(a) Concrete Masonry (Without Putty) (b) Clay Masonry (With Putty)

Figure 5. Influence of Amount of FRP Reinforcement

Figure 5 suggests that the lower limit ratio $M_{experimental} / M_{theoretical}$ for non-puttied masonry surfaces can be taken as 0.45; whereas for puttied surfaces this value can be 0.65. In addition, the index ω_f may be limited to 0.6 to prevent the occurrence of shear failure. These considerations can be taken into account for the implementation of a design methodology.

Conclusions

The following conclusions can be drawn from this experimental program:

- Strength and pseudo-ductility of URM walls can be substantially increased by strengthening them with FRP laminates. This increase can be observed in walls that can be idealized having simply supported conditions, such as walls with high h/t ratios (i.e. larger than 20), or in walls where the supports do not restrain the outward movement (i.e. arching mechanism is not observed)
- The test results made possible to identify three basic modes of failure. One, shear failure, related to the parent material (i.e. masonry); and two associated with the reinforcing material, debonding and flexural failure (i.e. rupture of FRP or crushing of the masonry). For large amounts of reinforcement (i.e. ω_f larger than 0.6), shear failure was observed to be the controlling mode. For other reinforcement ratios, either FRP rupture or debonding was observed, being the latter the most common
- Based on experimental data generated by the present investigation and others, it is recommended to consider the maximum usable strain in the FRP reinforcement as $0.45\varepsilon_{fu}$ for non-puttied surfaces and $0.65\varepsilon_{fu}$ for puttied surfaces

Acknowlegements

The support of the National Science Foundation Industry/University Cooperative Research Center at the University of Missouri–Rolla. The authors would also like to acknowledge the support of the Rolla Technical Institute (RTI).

References

1. Albert L.M., Elwi A.E., Cheng J.J., "Strengthening of Unreinforced Masonry Walls Using FRPs," ASCE Journal of Composites for Construction, Vol.5, No.2, May 2001, pp. 76-84.
2. American Concrete Institute (ACI), Committee 318, "Building Code Requirements for Reinforced Concrete and Commentary," American Concrete Institute, Detroit, Michigan, 1999.
3. American Concrete Institute (ACI), Committee 440, "Guide for the Design and Construction of Externally Bonded FRP Systems for Strengthening Concrete Structures," July 2000 (document under review).
4. Angel R., Abrams D.P., Shapiro D., Uzarski J., and Webster M, "Behavior of Reinforced Concrete Frames with Masonry Infills," Structural Research Series Report No. 589, Department of Civil Engineering, University of Illinois at Urbana-Champaign, March 1994.
5. Hamilton H.R. III, and Dolan C.W, "Flexural Capacity of Glass FRP Strengthened Concrete Masonry Walls," ASCE Journal of Composites for Construction, Vol.5, No.3, August 2001, pp. 170-178.
6. Masonry Standards Joint Committee, "Building Code Requirements for Masonry Structures," ACI-530-99/ASCE 5-99/TMS 402-99, American Concrete Institute, American Society of Civil Engineers, and The Masonry Society, Detroit, New York, and Boulder, 1999.
7. Roko K., Boothby T.E., and Bakis C.E., "Failure Modes of Sheet Bonded Fiber Reinforced Polymer Applied to Brick Masonry," Fourth International Symposium on Fiber Reinforced Polymer (FRP) for Reinforced Concrete Structures, Baltimore, Maryland, November 1999, pp. 305-311.
8. Tumialan J.G., "Strengthening of Masonry Structures with FRP Composites," Doctoral Dissertation, Department of Civil Engineering, University of Missouri-Rolla, Rolla, Missouri, 2001.
9. Velazquez-Dimas J.I., "Out-of-Plane Cyclic Behavior of URM Walls Retrofitted with Fiber Composites," Doctoral Dissertation, Department of Civil Engineering and Engineering Mechanics, The University of Arizona, Tucson, Arizona, 1998.
10. Wideman, B.A., "Mortar Cement Development in the United State," Proceedings of the 10th International Brick and Block Masonry Conference, Calgary, Canada, July 1994, pp. 1345-1354.
11. Yang X., "The Engineering of Construction Specifications for Externally Bonded FRP Composites," Department of Civil Engineering, University of Missouri-Rolla, Rolla, Missouri, 2001.